Carbohydrate Polymers 164 (2017) 13–22

Contents lists available at ScienceDirect

Carbohydrate Polymers

journal homepage: www.elsevier.com/locate/carbpol

Pectin-based composite film: Effect of corn husk fiber concentration on their properties

Dana C. Bernhardt[a,c], Carolina D. Pérez[b,c], Eliana N. Fissore[a,c], Maria D. De'Nobili[a,c], Ana M. Rojas[a,c,*]

[a] Departamento de Industrias, Facultad de Ciencias Exactas y Naturales, University of Buenos Aires, Ciudad Universitaria, C1428BGA, Buenos Aires, Argentina
[b] Instituto de Tecnología de Alimentos (ITA), INTA-Castelar, Buenos Aires Province, Argentina
[c] The National Research Council of Argentina (CONICET), Argentina

ARTICLE INFO

Article history:
Received 29 September 2016
Received in revised form
21 December 2016
Accepted 6 January 2017
Available online 11 January 2017

Chemical compounds studied in this article:
Arabinoxylans (PubChem CID: 6438923)
Carotene (PubChem CID: 5280489)
Lignin (PubChem CID: 73555271)
Polygalacturonic acid (PubChem CID: 445929)

Keywords:
Corn husk fiber
Pectin composite film
Antioxidant capability
Water vapor permeability
Tensile strength
Surface properties

ABSTRACT

Considering the polysaccharide composition and 32% of crystallinity of the water insoluble fiber extracted from corn husk (CHF) agricultural residue, its filler performance as water vapor permeability (WVP) and mechanical modifier in edible films based on commercial low methoxyl pectin (LMP) was evaluated (0, 1, 3, 5, 8% concentrations). The 53-μm-CHF carried phenolics and carotenes, and composites showed antioxidant capacity. Homogeneous films with a continuous LMP matrix were obtained. The 5%-CHF composite showed the highest surface contact angle (44°) and tensile strength, without change in elongation, while WVP was decreased in the 3–8% CHF-LMP-films. The latter was ascribed to the CHF-filler crystallinity whereas the improvement in mechanical performance and contact angle was attributed to a CHF-interconnected network formed at 5%-CHF critical concentration. Corn husk residue can be utilized as a source of fibers for material development. Composites with enhanced performance can be an antioxidant strategy at food interfaces.

1. Introduction

Maize (*Zea mays* L.; Poaceae family) is an angiosperm, monocot plant. When the corn grain is harvested, a stover remains as a by-product in the field. This residue consists of stalk, leaf, cob and husk tissues (Dhugga, 2007), which poses both disposal and environmental pollution problems though could yield valuable products (Olagunju, Onyike, Muhammad, Aliyu, & Abdullahi, 2013). Agricultural by-products are nowadays considered as a source of functional ingredients like antioxidants and dietary fibers (Galanakis, 2013). Also, the food industry and market gives rise to remnants that could be reused, since they are a good source of dietary fiber, functional oligosaccharides and phytochemicals.

Antioxidants are isolated from natural sources for food preservation (Shi, 2001) and they are also co-extracted with vegetable fibers, as reported by Larrauri, Rupérez and Saura-Calixto (1997) for mango peels. Polyphenols were found in the apple pomace remaining after juice extraction (Lavelli & Kerr, 2012), as well as in the inulin and pectin enriched fractions extracted from globe artichoke (Fissore et al., 2014). These fibers can be applied to material development such as biodegradable composite films.

The growing consumer demand for high quality and long shelf-life foods together with the concern about the use of synthetic

Abbreviations: AA, ascorbic acid; a_W, water activity; CHF, water insoluble corn husk fiber; DPPH, 2,2-diphenyl-1-picrylhydrazyl radical scavenging assay; DSC, differential scanning calorimetry; DTG, time derivative of thermal gravimetry; ERH, equilibrium relative humidity; FRAP, ferric reducing antioxidant power; FTIR, Fourier Transformed Infrared Spectroscopy; LMP, low methoxyl pectin; RH, relative humidity; SEM, Scanning Electron Microscopy; T_g, glass transition temperature; TGA, thermal gravimetric analysis; WVP, water vapor permeability.

* Corresponding author at: Departamento de Industrias, Ciudad Universitaria, C1428BGA, Buenos Aires, Argentina.
E-mail address: arojas@di.fcen.uba.ar (A.M. Rojas).

http://dx.doi.org/10.1016/j.carbpol.2017.01.031
0144-8617/

chemicals as food preservatives or an excessive use of them, have led to investigate about new strategies of food preservation. The biodegradable film covering a processed food can constitute other technological hurdle for food preservation because it is a barrier for gas diffusion while its microstructure can be used to carry, stabilize and localize the activity and control the release of preservatives (antioxidants, antimicrobials) at interfaces (De'Nobili, Pérez, Navarro, Stortz, & Rojas, 2013; Pérez et al., 2013). For edibility, polysaccharides and proteins have to be used for the film matrix development. They constitute very good barriers to gases like the deleterious oxygen, but not to water vapor. Nowadays, many research works seek decreased WVP in edible films, while mechanical properties are improved. Huq et al. (2012) produced by casting sodium alginate (3% w/v aqueous solution) films crosslinked by film soaking into 1% w/v $CaCl_2$ solution, reinforced with nanocrystalline cellulose (1–8% w/w on dry matter), which was obtained from a commercial bleached softwood kraft pulp. The WVP of films (25 °C; 0%–60% relative humidity, RH, gradient) decreased as the nanocrystalline cellulose concentration increased from 0% (6.37×10^{-11} g m^{-1} s^{-1} Pa^{-1}) to 8%w/w (4.05×10^{-11} g m^{-1} s^{-1} Pa^{-1}) in the alginate films, while the tensile strength of 56%RH-equilibrated films increased almost linearly from 57 MPa for 0%- up to a maximum of 78 MPa for 5%-nanocrystalline cellulose, whereas higher concentrations (8%) did not increase the tensile strength (75 MPa). Conversely, the relative elongation reached at film rupture decreased continuously from 10% to 4.8% for 0 and 8% w/w nanoparticle contents, respectively, in the alginate films. Shekarabi, Oromiehie, Vaziri, Ardjmand and Safekordi (2014) determined that loading nanoclay (non edible) particles (0.5, 1, 1.5 and 2 g/100 g quince seed) in films casted from heated aqueous solutions of quince seed mucilage (10% w/w), plasticized with polyethylene glycol (5 g/100 g polymer), decreased the WVP (0%/52%RH gradient; 25 °C) of films from 1.86×10^{-10} to 0.306×10^{-10} g m^{-1} s^{-1} Pa^{-1}, during a month of film storage. Also, enhanced the tensile strength from 16 to 22 MPa while the relative elongation increased from 2.48% to 6.5%, when measured at 2 mm/min. Andrade, Ferreira, & Gonçalves (2016) casted edible films from the solid residue of whole fruits and vegetables (e.g. orange, watermelon, lettuce, courgette, carrot, spinach, potato skins) processed into flour and suspended in water (8 and 10% w/w) for film forming solution. Films were stored at 0% RH until characterization. Their WVP (0/100% RH gradient; 25 °C) varied between 6.81 and 7.72×10^{-10} g m^{-1} s^{-1} Pa^{-1}. The tensile strength at film fracture increased from ≈ 27 kPa to 70–84 kPa with the addition of flour potato skins, all accompanied by a 30.5–34.5% of elongation.

By considering the chemical composition before determined by Bernhardt, Ponce, Stortz and Rojas (2015), the water insoluble fiber (CHF) extracted from corn husk of maize industrialization was proposed as filler to decrease the WVP of calcium-crosslinked LMP films, together with an improvement in the surface characteristics and mechanical strength, while antioxidant capacity can also be associated. Being then necessary to determine the optimal CHF concentration to be loaded in films, 0, 1, 3, 5 and 8% of CHF levels were evaluated in the present work to determine the effect of CHF on the performance of the composite films.

2. Materials and methods

2.1. Chemicals

Deionized water was used (MilliQ, Millipore, USA). Food grade pectin with a low degree of methyl esterification (GENU™ pectin type LM-12 CG) was a gift from CP Kelco (Denmark). Sucrose (34.3% w/w) is added by the manufacturer for standardization, as determined by De'Nobili et al. (2013). The pectin content of this product is characterized by a mean molecular weight of 734.2 kDa and a D-galacturonic acid content of 85% w/w, which is 40% methylesterified and 6.0% acetylated (De'Nobili et al., 2013). The rest of the pectin molecules are constituted by rhamnogalacturonan components such as L-rhamnose, D-galactose and low level of arabinose. Potassium sorbate, DPPH (2,2-diphenyl-1-picrylhydrazyl), TPTZ (2,4,6-tripyridyl-s-triazine), and $FeCl_3 \cdot 6H_2O$ were from Sigma–Aldrich (Saint Louis, USA). Glycerol, $CaCl_2 \cdot 2H_2O$, $CaCl_2$ anhydrous, $MgCl_2$, NaBr, NaCl, methanol, acetone, L-(+)-ascorbic acid, gallic acid, Folin reagent, acetic acid, sodium acetate, hydrochloric acid, carbon tetrachloride, and *n*-heptane were of analytical quality from Merck (Argentina).

2.2. Water insoluble fiber (CHF) extraction

Corn (*Zea mays* L.) husks discarded by canning industry and green groceries were collected. They were the green, light green and slightly yellow colored outer shells. Husks were dried at 65 °C for 4 h under high air convection in order to obtain completely dried husks, which showed a brittle texture. Dried husks were transversally cut into strips of ≈15 mm-width and then milled through a cutting mill (Heavy-Duty Cutting Mill SM 300, Retsch, Germany) provided with a 500 μm mesh sieve. A weighed corn husk powder sample was submitted to extraction with deionized water (1:100 w/v) at 25.0 °C for 24 h under magnetic stirring. Afterwards, the dispersion was filtrated through a glass filter membrane (Whatman GF/C, UK) and washed three times with water by re-dispersion, followed by filtration. The final solid residue (water insoluble fiber) was frozen and freeze-dried. This water insoluble fiber was then classified by particle size. Weighed amounts were sieved through a vibratory sieve shaker (Retsch, Germany) provided with 840, 420, 210, 105, 53, 25 μm ASTM mesh sizes. The fraction recovered between the two closest sieves was weighed for yield calculation and stored under vacuum in hermetically sealed pouches. The 53 μm water insoluble fiber, called "CHF", was used for films.

2.3. Film preparation

According to the CHF concentration to be considered (0.0, 1.0, 3.0, 5.0 or 8.0 g per 100 g of LMP) for film making, a weight of 0, 0.0525, 0.1575, 0.2625 and 0.4200 g of CHF were respectively dispersed in 25.00 mL of deionized water, mixed through a vortex for complete humectation and left for 18 h. On the other hand, 8.00 g of the commercial GENU™ pectin containing 5.25 g of LMP was dispersed in ≈250.00 g of deionized water under continuous controlled high-speed shear (1400 rpm-constant) stirring performed with a vertical stirrer (LH, Velp Scientifica, Italy) for homogeneous hydration of the pectin powder. After heating to 90 °C (5 °C/min) under stirring, potassium sorbate (0.0900 g) and glycerol (2.4000 g) plasticizer were added, previously dissolved and dispersed in ≈10 mL of deionized water. The CHF dispersion (25.00 mL) of a given CHF concentration was then added to the film making solution while stirring, followed by 0.5000 g of $CaCl_2 \cdot 2H_2O$ pre-dissolved in ≈5 mL of deionized water, maintaining the system at 85 °C. The total weight of the film making solution was then made 300.00 g by addition of enough deionized water and homogenized (De'Nobili et al., 2013). This hot solution was placed under vacuum for 20 s to remove air bubbles and poured in a constant weight onto horizontally leveled and numbered polystyrene plates (200 × 200 mm). After cooling at room temperature (23 °C) for gelling, drying was performed (60 °C, 3 h) under forced convection. Films were then peeled off and stored hanged under vacuum (25.0 °C) over NaBr saturated solution (water activity, $a_W^\circ = 0.577$) into chambers, in order to maintain a constant RH (57.7%) for film equilibration (Eq. (1)) (Greenspan, 1977).

Three batches of films (triplicate) for each CHF concentration (0.0, 1.0, 3.0, 5.0, 8.0%) studied were produced as explained, and films obtained were numbered.

Film a_W was daily measured in triplicate at 25.0 °C through a Decagon AquaLab (Series 3 Water activity meter, USA), in order to determine the time at which the film equilibration was attained, called equilibrium relative humidity (ERH) (Eq. (1)).

$$a_W = {}^{ERH}/_{100} \quad (1)$$

2.4. Film characterization

The following assays were performed on at least one film sample from each batch after the ERH (57.7%) was reached (Eq. (1)).

2.4.1. Antioxidant capacity and total phenolic content of films

Each film sample carefully cut into pieces smaller than 1 mm in size, and weighed (3.0000 g) on an analytical scale (0.0001 g), were sonicated for 15 min with 20.0 mL of extractive solution (acetone/water/acetic acid; 70:29.5:0.5 (v/v/v)), as explained by Basanta et al. (2016). The homogenates were then centrifuged at 4000 × *g* for 10 min at 6 °C (Eppendorf 5804 R, Germany). The acetone was evaporated at 35 °C under vacuum (Rotavap Büchi, Germany). The aqueous residue was filtered through an activated Sep-Pack C-18 solid phase extraction cartridge (Waters, Milford, MA, USA), washed with water and the retained phenolic compounds were then eluted with 1.000 mL of methanol.

Aliquots of the 1.000-mL-methanolic extract obtained from each film were then evaluated in their respective radical scavenging activity through the DPPH (2,2-diphenyl-1-picrylhydrazyl) assay, and ferric reducing antioxidant power (FRAP). The DPPH assay was carried out according to Brand-Williams, Cuvelier, and Berset (1995). The FRAP test was performed as explained by Pulido, Bravo and Saura-Calixto (2000). Results were expressed as L-(+)-ascorbic acid (AA), the standard used in both methods, whose calibration curves were developed with the standard dissolved in methanol.

The 1.000-mL-methanolic extract eluted from the Sep-Pack C-18 cartridge after the extraction of other film sample of a given CHF concentration was completely evaporated under a nitrogen stream. The dried residue was then dissolved in HCl (pH < 2) for determination of the total phenolic content through the Folin-Ciocalteau technique, according to Shui and Leong (2006). Gallic acid was used as standard and the results were expressed as mg of gallic acid per 100 g of film sample.

Determinations were performed in triplicate.

2.4.2. Film color

Measurement of *L*, *a*, and *b* (HunterLab) film color parameters was performed with a Minolta colorimeter (Minolta CM-508d, Tokyo, Japan) (Idrovo Encalada, Basanta, Fissore, De'Nobili, & Rojas 2016).

2.4.3. Moisture

Water content of film samples cut in 1-mm pieces was determined by drying under vacuum at 70 °C up to constant weigh (≈26 d). Moisture was determined in triplicate, and then calculated and expressed per 100 g of dry mass.

2.4.4. Glass transition temperature (T_g)

Modulated differential scanning calorimetry (MDSC, TA Instruments, USA) was used to determine the T_g (midpoint temperature) as the first derivative of the heating ramp recorded from the second scan performed on an equilibrated film sample (10–15 mg) or CHF powder loaded into a hermetically sealed alumina pan (De'Nobili et al., 2013).

2.4.5. Thermal gravimetric analysis (DSC-TGA)

Thermal decomposition of CHF and films was separately performed through a simultaneous thermal analyzer (TG-DSC/DTA, TA Instruments SDT Q600, USA). Each sample (≈10 mg) placed in an alumina pan was thermally treated under flowing N_2 (100 mL/min) from ambient temperature to 600 °C, at 10 °C/min-heating rate. The mass loss and calorific changes as a function of temperature were then recorded and used to plot the TG and derivative thermogravimetric (DTG) curves. Experiments were performed in triplicate.

2.4.6. X-ray diffraction

A Philips X-ray diffractometer with vertical goniometer was used (Cu Kα radiation λ = 1.542 Å) and operation was performed according to De'Nobili et al. (2013). Distances between the planes of the crystals *d* (Å) were calculated from the diffraction angles (°) obtained in the X-ray pattern, according to the Braggís law:

$$n\lambda = 2d \sin\left(\theta\right) \quad (2)$$

wherein λ is the wavelength of the X-ray beam and *n* is the order of reflection, which was considered as 1 for calculation. Degree of crystallinity was calculated according to Xiao, Sun, Shi, Xu and Sun (2011).

2.4.7. Fast Fourier Transformed Infrared Spectroscopy (FTIR)

FTIR spectra were recorded at ambient temperature and atmospheric pressure on a Nicolet 8700 (Thermo Scientific Nicolet, MA, USA) spectrometer, which was equipped with a diamond attenuated total reflection (ATR) device, a DTGS TEC detector, and a reflection incident angle of 45°. Each spectrum was obtained by recording reflectance (%) through 64 scans performed with a resolution of 4 cm^{-1} and between 4500 and 525 cm^{-1}. Spectra were analyzed through the OMNIC software (version 7.3, Thermo Electron Corp., United States).

2.4.8. Film density

The film density was determined for each CHF concentration studied using the floatation method with carbon tetrachloride (1.588 g/ml) and *n*-heptane (0.693 g/mL), at 25.0 °C, as explained by Singh, Chatli and Sahoo (2015).

2.4.9. Water vapor permeability (WVP) of films

It was determined and calculated according to the Gennadios, Weller and Gooding (1994) correction for hydrophilic films. Film sample was placed between the anhydrous calcium chloride in the cup container and the 70% RH environment, at 25 °C (Ibertest chamber, Spain).

2.4.10. Tensile assays

57.7%RH-equilibrated film sample strips (25.0 mm × 6.0 mm) with parallel sides were cut with a cork borer and each probe was submitted to a uniaxial tensile assay until film rupture (5 mm/min-constant crosshead speed), using an Instron Testing Machine (model 3345, Norwood, MA, USA) provided with a 100 N load cell and pneumatic clamps with parallel faces coated with rubber. Film thickness was measured with a digital micrometer (Mitutoyo, Kawasaki, Japan) to the nearest 0.001 mm at three different locations of the specimen before performing each tensile assay.

Force (N)-elongation (m) curves were recorded and the normal stress (σ_{break}) and strain (ε_{break}) at film rupture were respectively calculated as:

$$\sigma_{break} = F_{break}/A_O \quad (3)$$

$$\varepsilon_{break} = (L_{break} - L_O)/L_O \quad (4)$$

wherein A_O is the initial cross sectional area of the film sample; L_O is the initial gap between the clamps that maintained fixed the film

probe with a pre-load of 0.1 N; F_{break} is the film force and L_{break} is the film length both reached simultaneously at film rupture.

At least fourteen replicates of strips were measured for each CHF concentration.

2.4.11. Contact angle

It was tested through the sessile drop (0.0040 mL) deposited at three representative areas of each horizontally leveled film surface (three film samples per system studied) using a contact angle goniometer (NRL Contact Angle Goniometer, model 100-00, Rame-Hart, USA) (Idrovo Encalada et al., 2016).

2.4.12. Scanning electron microscopy (SEM)

For morphological characterization, films were cut in rectangular pieces of about 9 × 40 mm, fractured under immersion in liquid nitrogen and then mounted vertically on the stationary support for observation of the fractured cross-section and surface morphologies. Samples were then gold-coated in a chamber under high-vacuum, and afterwards placed into the chamber of a FEI Quanta 250 FEG Scanning Electron Microscope (Thermo Fischer Scientific, USA). Images were acquired under high-vacuum, at an accelerating voltage of 3 kV and using an ETD detector for secondary electrons.

2.5. Statistical analysis

Results were informed as the average and standard deviation for n replicates of each sample, after analyzed through ANOVA (level of significance, $\alpha = 0.05$) followed by multiple comparisons evaluated through the least significant difference test (Statgraphic Plus for Windows, version 5.0, 2001, Manugistic Inc., USA).

3. Results and discussion

3.1. CHF

The dried corn husks reduced through a cutting mill to a powder produced a 69 ± 1% w/w of water insoluble fiber (CHF). It was characterized by 15.9, 55.4, 18.2, 8.7 and 1.9% w/w of 420, 210, 105, 53 and 25 μm average particle sizes, respectively. The 53 μm-fraction of CHF was assayed as filler to develop the composite films. As previously determined by Bernhardt et al. (2015), CHF was enriched in the cell wall polymers composed by polysaccharides (80% w/w, dry basis), proteins (13.2%) and ≈8% of lignin. Also, total phenolics (2.64 g/100 g CHF) and carotenes (5.74 mg/100 g CHF) were found. An antioxidant capacity of 25–33 mg/100 g CHF, expressed as AA, was determined, which can be associated to the phenolics and carotenes. Polysaccharides included 5.5% w/w of pectins, 26.21% w/w of hemicelluloses (essentially arabinoxylans), 26% w/w of cellulose and a 0.58% of total starch. A 32% of crystallinity was determined through X-ray diffraction by Bernhardt et al. (2015) for the CHF.

3.2. Film characteristics

Arabinoxylan, cellulose and lignin contents (≈60%) together with a very low pectin level and a 32% of crystallinity permitted to infer a lower hydrophilic character for the CHF, being then proposed as a filler to increase the barrier properties to water vapor of an edible film based on calcium-crosslinked LMP (8.58×10^{-4} moles of Ca^{2+}/g pectin). The 53 μm-CHF was loaded at concentrations between 0 and 8 g per 100 g of LMP polymer. A proportion of 15.2 g of glycerol per 100 g of LMP was used for plasticization to obtain films with adequate flexibility.

All casted films obtained after drying were flexible and composites were also resistant to handling, showing uniformly dispersed particles at all CHF concentrations assayed. The ultrastructure revealed through the SEM technique showed a homogeneous and completely smooth, flat surface in the LMP film samples made without CHF (0% w/w) (Fig. 1A). On the other hand, composite films loaded with CHF at concentrations of 5% (Fig. 1B) or 8% w/w (Fig. 1C) also showed the homogeneous surface of the continuous LMP matrix but furrowed by increasing number of channels or depressions, with the appearance of some rough small regions in the 8%-CHF composite film. The cross-section of 0%-CHF LMP film was very compact, smooth, and in general flat, also showing smooth and clearly defined borders (Fig. 1-A1). The 5%-CHF composite film showed the homogeneous, smooth and continuous LMP matrix, but CHF structures were observed as tubes emerging as a consequence of the film fracture under nitrogen (Fig. 1-B1; black arrows). Wavy, smooth, well defined borders were observed in the composite, where a white arrow pointed a superficial wave of polymer film that covered a protruding fiber. As specially observed in the 8%-CHF composite film, the superficial waves (Fig. 1-C1; black arrow) that were responsible for the surface morphology with channels or depressions (Fig. 1C), were produced by the CHF tubes (Fig. 1-C1; black arrow) and other fiber particles (Fig. 1-C1; white arrow) immersed in the continuous LMP matrix. CHF particles increased locally the film thickness.

The Hunter Lab color parameters of films are shown in Fig. 2. It can be observed that the high value of lightness (L) determined for films without fibers (0%-LMP film) was in general maintained when the CHF was loaded (Fig. 2A). At this L level, the a values of films were negative, that is, tended towards greenness, being similar for 0%-LMP and 5%-composite films (Fig. 2B). The b values were positive and, hence, shifted to yellowness, which tended to increase significantly ($p < 0.05$) with the CHF particle concentration, probably due to the carotenes present in the CHF (Fig. 2C).

The casted composites reached the 57.7%-RH equilibrium in a considerably longer period (>2 weeks) of storage than in the case of 0%-LMP film (≈48 h). Hence, the presence of CHF constituted a barrier for water adsorption by the pectin network. After equilibration (Eq. (1)), the corresponding moisture contents and T_g were determined, as well as the film thickness, WVP and mechanical performance, X-ray diffraction and FTIR analysis.

For the same weight of film forming solution poured into each plate for casting, the film thickness was significantly ($p < 0.05$) higher for 3–8% than for 0–1% CHF concentrations (Fig. 3A). Thus, the increment was due to the volume occupied by the CHF loaded, as can be observed in the SEM images (Fig. 1, B1 and C1). The film density significantly ($p < 0.05$) decreased for CHF concentrations above 1% w/w in the composite films, with no difference between 5% and 8% of CHF (Fig. 3B). Film density values varied between 1.993 ± 0.070 g/cm^3 for the 0%-CHF LMP film, and 1.516 ± 0.040 and 1.481 ± 0.090 g/cm^3 for the 5%-CHF and 8%-CHF composite films, respectively. Ramos et al. (2013) determined values of density between 1.26 and 1.38 g/cm^3 for films based in whey protein isolate and whey protein concentrate. Singh et al. (2015) found values between 1.371 and 1.431 g/cm^3 for films made with different chitosan and glycerol (plasticizer) proportions.

The moisture content was not significantly different ($p < 0.05$) between films (Table 1). The T_g values were below the 25.0 °C storage temperature (Table 1), which indicated that all equilibrated films were at the amorphous rubbery state at room temperature, demonstrating a significant macromolecular mobility due to the plasticization produced by glycerol and the adsorbed water. DSC scans of LMP based films did not show an endothermic peak at 0 °C, which corresponds to freezable (available) water. It meant that the water adsorbed at 57.7% RH was strongly retained by the LMP-film matrix (Hatakeyama & Hatakeyama, 1998; Träubel, 1999), e.g. at the calcium crosslinks, which coordinate with water molecules (Braccini & Pérez, 2001; Ping, Nguyen, Chen, Zhou, & Ding, 2001).

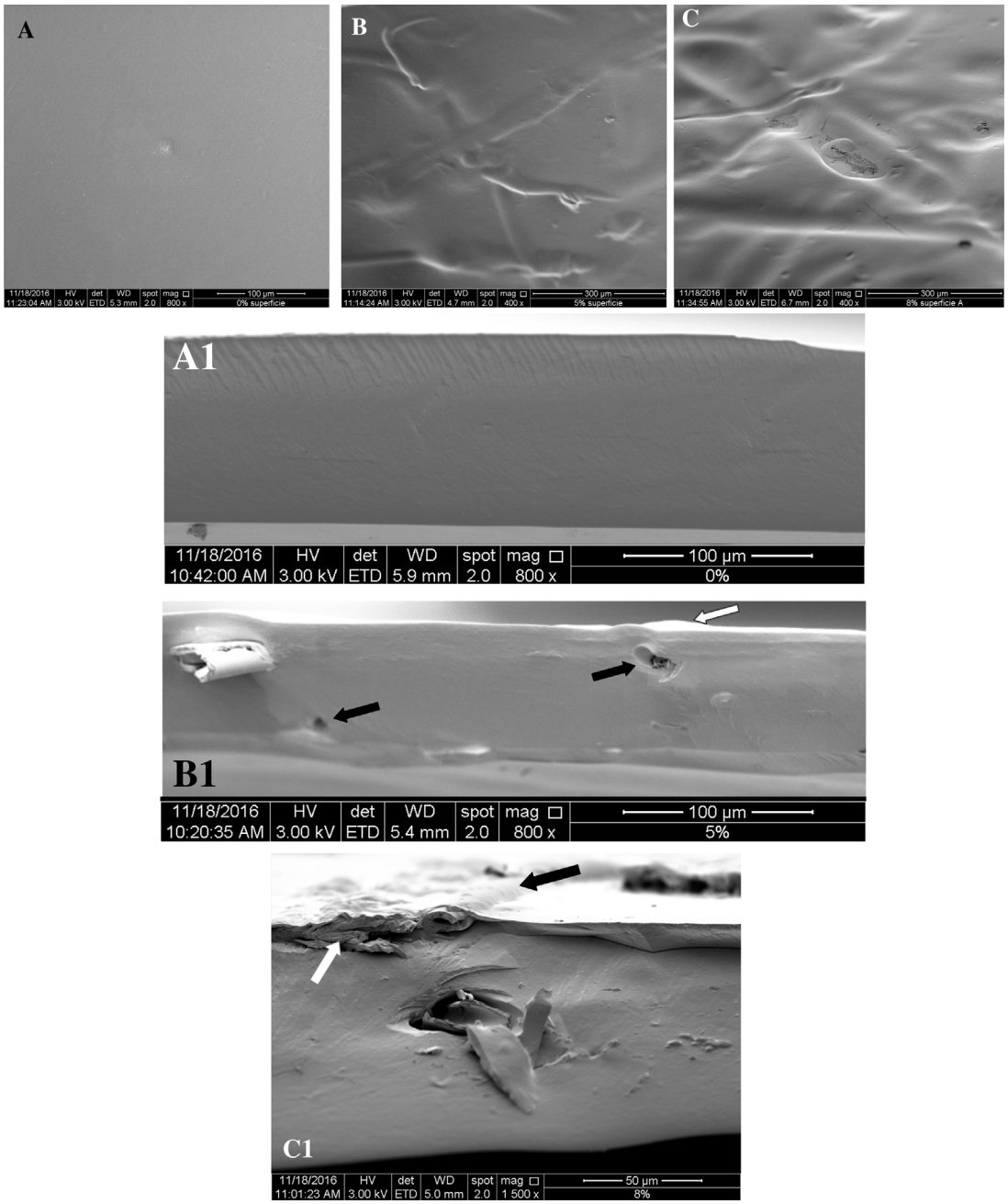

Fig. 1. Surface morphology of LMP films made without (A) or loaded with 5% (B), and 8% w/w (C) of CHF, and their respective cross-sections (A1, B1, C1).

Table 1
Moisture content and glass transition temperature (T_g) of films.

	Composite films (% w/w corn husk fiber)				
	0	1	3	5	8
Moisture content[a,b] (g/100 g dm)	26 ± 2 [A]	24.8 ± 0.6 [A]	25.2 ± 0.4 [A]	24.2 ± 0.3 [A]	27 ± 5 [A]
T_g (C)	−64.89	−66.78	−68.42	−71.83	−67.50
	–	–	+109.53	+109.58	+89.55
					+109.56
Change in specific heat at the glass transition [J g^{-1}(dm) K^{-1}]	3.701	3.824	3.746	2.690	4.062
	–	–	4.830	4.862	4.718
					4.885

dm: dry mass.
[a] Mean and standard deviations for $n = 3$ are reported.
[b] The same capital letter as superscript of data in a given row means non significant differences ($p<0.05$).

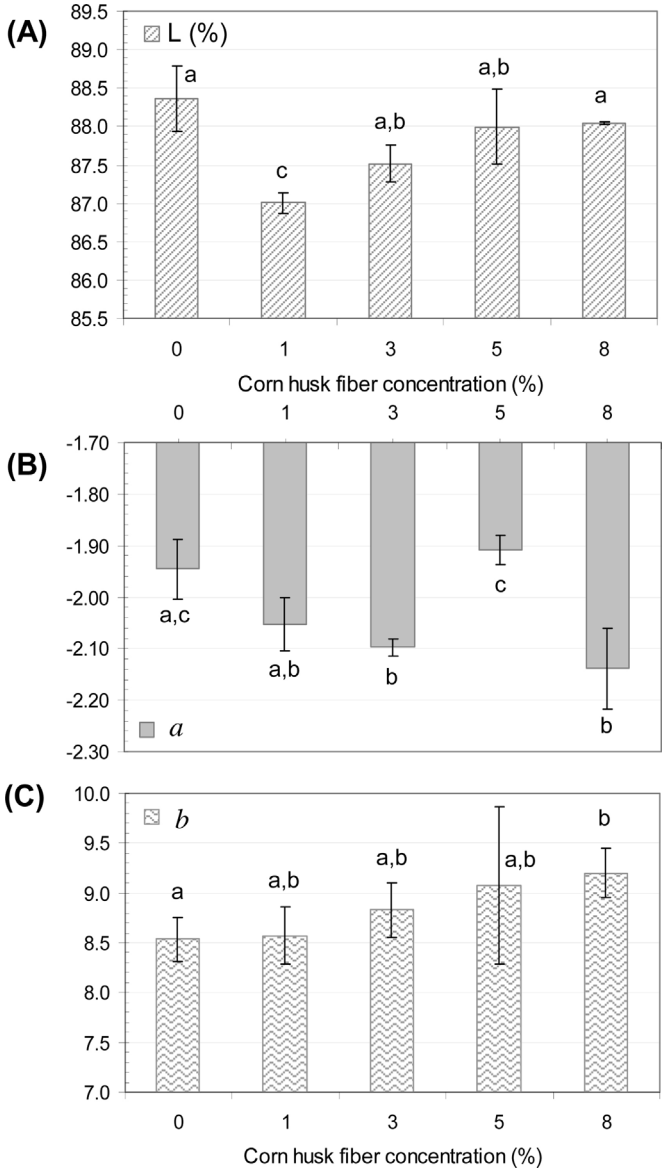

Fig. 2. Hunter Lab color parameters of films: lightness, L (A), as well as a (B) and b (C). Error bars indicate the standard deviation ($n > 12$). The same letters for a given parameter mean non significant differences ($p < 0.05$).

Since films are composites, other T_g values associated to the CHF particles can be expected. A second T_g was detected at ≈109.58 °C (≈4.8 J g^{-1} K^{-1}; Table 1) for 3%, 5% and 8% CHF-composite films. CHF isolated powder showed T_g values at 30.28 °C (0.354 J g^{-1} K^{-1}), 53.59 °C (0.747 J g^{-1} K^{-1}) and 109.39 °C (3.110 J g^{-1} K^{-1} on dm), being the latter also found in the CHF-composite films (Table 1). It was interesting to observe a third T_g value (89.55 °C) only in the 8% CHF-composite film. T_g values above the room temperature (25.0 °C) indicate that the amorphous regions of the CHF-composite films are heterogeneous, part of which are at the glassy state, associated to the CHF filler particles (Liu, Bandhari, & Zhou, 2006).

3.3. FTIR analysis of films

The FTIR study was performed on film surfaces through ATR. In this way, the characteristic spectrum of the LMP polymer plasticized by glycerol was essentially observed in the FTIR spectra recorded from all film systems herein studied (Fig. 4). It was inferred by comparison with the spectrum recorded from a film

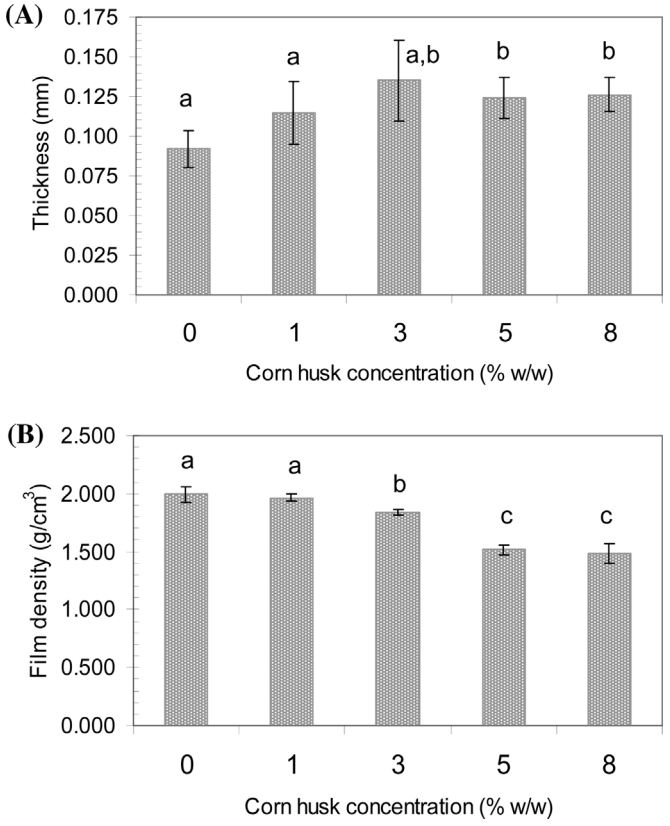

Fig. 3. Thickness of 57.7%-RH equilibrated films (A) and film density (B) plotted against CHF contents. Error bars indicate the standard deviation ($n > 3$). The same letters for a given parameter mean non significant differences ($p < 0.05$).

made only with the LMP polymer and equilibrated at 0% RH (Fig. 4). Both the band intensity and width recorded at ≈3297 cm^{-1} of wavenumber decreased as the CHF concentration increased in the film network (Fig. 4). This is a broad typical band ascribed to intra and intermacromolecular hydrogen bindings of polysaccharide macromolecules from cell walls (Coimbra, Barros, Barros, Rutledge, & Delgadillo, 1999). When compared to the spectra obtained from the 0%-RH (anhydrous) LMP film, considerable higher peak intensity can be observed in 57.7% RH-equilibrated films (Fig. 4).

In the spectra recorded from the 0%-RH LMP film, the broad shorter band at 2942 cm^{-1}, corresponding to the OH-stretching in the carboxylic groups of pectins, was observed, whereas in the FTIR spectra of 57.7%-equilibrated films, this band showed the peak at 2942 cm^{-1} and other at 2896 cm^{-1}, both typical of glycerol. This band did not change with the CHF concentration (Fig. 4). The intensity of the 1654 cm^{-1} band, which corresponded to the water deformation band of water adsorbed (δ HOH) on polysaccharides (Wilson et al., 2000), also seemed to be profoundly affected by the CHF concentration dispersed in the LMP films (Fig. 4). This fact can demonstrate the obstacle that CHF exerted on the water adsorption by the LMP macromolecules of film matrix, even at the same water activity of films. In the 0%-RH LMP film, the absence of adsorbed water revealed the band that corresponded to the ionized carboxylate group, band slightly shifted to higher wavenumbers (from 1630 to 1654 cm^{-1}) because the compounds are in the solid state (Assifaoui, Loupiac, Chambin, & Cayot, 2010).

On the other hand, the peak recorded at 1749 cm^{-1}, attributed to the C=O stretching of the esterified carboxyl group of pectins, was not affected by the CHF presence (Fig. 4), neither by the absence of water adsorbed in the 0%-RH LMP film (Fig. 4).

The intensity of the three peaks and shoulder recorded between 1101 and 1018 cm^{-1}, characteristics of the polygalacturonic

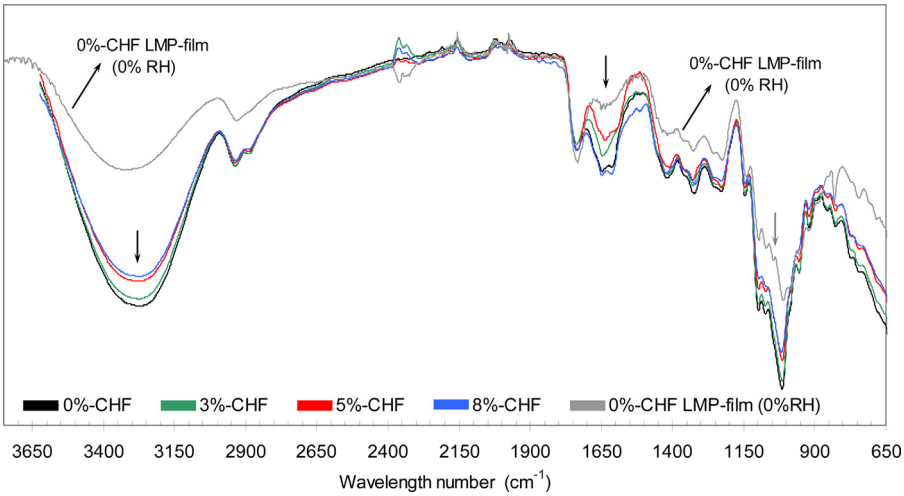

Fig. 4. Transmission FTIR spectra recorded through ATR from LMP films made without (0%) or loaded with CHF (1–8%), equilibrated at 57.7% RH, as well as from 0% CHF-LMP film equilibrated at 0% RH.

backbone in the fingerprint zone (1200 to 900–850 cm^{-1}) of pectins, decreased as the CHF concentration increased (Fig. 4). In the spectrum recorded from the 0%-RH LMP film, a fourth peak at 1049 cm^{-1} and other at 998 cm^{-1} can be clearly observed (arrow; Fig. 4), which disappeared in films plasticized by glycerol and equilibrated at 57.7% RH, due to the broadening produced by the hydrogen bonding of the plasticizers to the pectin polymer. Stable hydrogen bonds may be formed between glycerol plasticizer and the O atom in the C—O covalent bond of pectin polymers (Yang, Yu, & Ma, 2006). It is showed by the broadening at 1018 cm^{-1} as well as by the band shift of the OH-stretch from 3332 to 3297 cm^{-1}.

3.4. Composite film performance

3.4.1. Thermal stability

DSC scanning under N_2 of the CHF isolated powder showed an endotherm at 174.70 °C (92.5 J/g dry mass), which can correspond to a phase transition such as fusion of crystalline regions. Also, an exothermic peak at 274.86 °C (102.1 J/g dry mass) was observed, probably associated to hemicellulose and cellulose decompositions.

Under nitrogen, the thermal scan obtained through TGA from the CHF powder was characterized by higher temperatures of polymer decomposition than those obtained from the thermal scans of films (Table 2). The onset for thermal decomposition of films increased significantly in temperature ($\Delta T \geq 10$ °C) with the presence of CHF (Table 2). Above this, the film profiles showed two inflexion points, which were revealed by the two peaks observed in the time derivative of TG (DTG). The first peak, determined at 160 °C for the 0%-LMP film and 147–155 °C range for the composite films (Table 2), may correspond to elimination of highly adsorbed water. The second peak occurred at 238–244 °C range, which can correspond to decomposition of polysaccharides, accompanied by a mass loss that varied between 29.2 and 41.7% (Table 2). In the case of wheat straw, the hemicellulose fraction, comprising about 75% of the hemicellulosic material, was isolated from the delignified material by Fang, Sun and Tomkinson (2000). It consisted mainly of arabynoxylans and a minor amount of residual lignin. The degradation of this fraction started at 220 °C and was completed at around 395 °C.

Afterwards, between 281° and 301 °C (Table 2), the polymer degradation, probably lignin, continued up to 600 °C. Cellulose, in its microcrystalline form, has been reported as beginning its thermal degradation (onset) at ≈315 °C, while the maximum of decomposition in the DTG was observed at 370 °C, for 10 °C/min of scanning velocity (Huang, 2012).

3.4.2. X-ray diffraction studies

For comparison, Fig. 5A shows the X-ray diffraction pattern of the 53 μm-CHF powder, with a calculated 32% degree of crystallinity. A characteristic amorphous profile was observed with only a detectable intensity in the region at $2\theta \approx 14.325$ (sharp signal; d spacing, ≈6.18 Å; Eq. (2)), accompanied by an amorphous region that can be ascribed to xylans and cellulose, at values of 2θ between 10 and 18 (Uhlin, Atalla, & Thompson, 1995).

The LMP film without CHF showed an amorphous profile (Fig. 5B), as also observed in Fig. 1A. Ordered regions of the LMP network crosslinked by calcium ions were completely plasticized by glycerol and the water vapor adsorbed. A similar amorphous pattern was shown by the 5%-CHF LMP-composite, but a detectable intensity was observed in the region at $2\theta \approx 14.985$ (d spacing, ≈5.913 Å; Eq. (2)) (Fig. 5C). Well-ordered binding in the polysaccharide component of CHF-LMP film was not totally eliminated by network plasticization. Actually, the composite microstructures were heterogeneous, and ordered crystalline regions of CHF (Fig. 5C, arrow) were distributed among the amorphous regions of the LMP-plasticized network (Fig. 1B, C), as revealed by T_g results (Table 1).

3.4.3. Mechanical properties and water vapor permeability (WVP)

Uniaxial tensile assays until fracture of 57.7%-equilibrated films (Fig. 6A) showed that the strength at failure (Eq. (3)) of 5%-CHF composite (141 MPa/-) was significantly ($p < 0.05$) higher than the values obtained from the other films (≈60–70 MPa). The 1%- and 8%-CHF composites showed strength values significantly ($p < 0.05$) lower than those determined for 0%- (≈ 90 MPa) and 5%-CHF films (Fig. 6A).

The relative elongation at break (normal strain; Eq. (4)) was ≈9%, being not significantly different between the film systems studied (Fig. 6B). Hence, it can be inferred that the degree of plasticization produced by glycerol and water on the film networks seemed to be similar, even though the glycerol proportion loaded was calculated on the LMP polymer basis. As relative elongation was not different, the calculated values of strength at film break (Fig. 6A) can be directly related to the corresponding values of recorded force and calculated stress at film fracture.

Table 2
Thermal gravimetric analysis of films. The corresponding weight loss is informed in parentheses.

Temperatures	Corn husk fiber powder[a]	Composite films (% w/w corn husk fiber)				
		0	1	3	5	8
Onset of 1st peak (C)	197° (3.52%)	112° (6.88%)	124° (8.59%)	128° (17.72%)	123° (7.97%)	121° (9.55%)
1st peak (C)	304° (26.99%)	160° (12.5%)	154° (12.0%)	147° (20.4%)	155° (12.45%)	149° (13.48%)
End of 1st peak (C)	329° (39.15%)	184° (16.34%)	184° (15.4%)	174° (23.9%)	173° (14.4%)	171° (15.73%)
2nd peak (C)	352° (52.97%)	238° (29.7%)	240° (29.2%)	243° (41.7%)	239° (29.3%)	244° (32.0%)
End of 2nd peak (C)	393° (65.08%)	289° (41.3%)	285° (39.5%)	290° (53.2%)	281° (39.8%)	301° (44.9%)

[a] Water insoluble fiber.

Table 3
Contact angle[a] measured at 5 and 60 s of contact with the water drop at the film surface.

	Composite films (% w/w corn husk fiber)				
	0	1	3	5	8
Contact angle[b] (°) at 5 s	25 ± 3^{A}	24 ± 9^{A}	25 ± 3^{A}	44 ± 8^{B}	23 ± 2^{A}
Contact angle[b] (°) at 60 s	21 ± 2^{A}	18 ± 9^{A}	21 ± 4^{A}	36 ± 9^{B}	19 ± 4^{A}

[a] The arithmetical average and standard deviation ($n = 9$) are reported.
[b] The same capital letter as superscript of data in a given row as well as into a column means non significant differences ($p<0.05$).

Table 4
Phenolic content and antioxidant capability of films determined through the radical scavenging (DPPH) and reducing (FRAP) activities.

Fiber content of films (% w/w)	Total phenolic content[a,b] (mg/100 g film)	Antioxidant capacity	
		DPPH[a] (mg AA/100 g film)	FRAP[a] (mg AA/100 g film)
0	18 ± 2^{A}	ND	ND
1	102 ± 26^{B}	ND	17.6 ± 0.2^{A}
5	149 ± 14^{B}	ND	25 ± 6^{B}
8	254 ± 16^{C}	16 ± 6	29 ± 2^{B}

The same capital letter as superscript means non significant differences between treatments in the same column.
ND: non detectable.
[a] The arithmetical average and standard deviation ($n = 3$) are reported.
[b] Expressed as gallic acid.

For 1% and 3% of CHF-particle contents, the decrease in the force at rupture and, hence, in the strength at failure (Fig. 6A), can probably indicate that a low number of particles distributed in the pectin matrix behaved as heterogeneities and, hence, points of failure for the polymeric (LMP) matrix. A fully dispersed stage of CHF particles in the LMP matrix is formed, which can not dissipate the stress (Wessling, 1991). The 5%-CHF concentration seemed to be the ideal for mechanical resistance and, hence, it is the critical particle volume fraction. This volume fraction is determined by the interfacial energy at which the isolated primary particles are closer to each other and could probably flocculate, forming an interconnected network (Wessling, 1991). This network of microparticles could be developed, whatever their shape. The corresponding surface morphology is shown by Fig. 1B. At 5% concentration, the 53-μm CHF-particles behaved as a reinforcing filler material, making the strongest film. CHF concentrations above 5% (e.g. 8%) may not be well distributed between LMP strands when the film network is developed during casting, probably due to particle aggregation. Fig. 1C revealed the underneath higher fiber distribution, while Fig. 1-C1 shows the significant higher presence of fibers in the 8%- than in the 5%- CHF composite film.

Beyond the mechanical behavior observed, CHF contents above 1% decreased significantly ($p < 0.05$) the WVP of films with respect to the 0%-LMP film, when evaluated at 25 °C under convection in a 0%-70% RH gradient, after applying the correction of Gennadios et al. (1994) (Fig. 6B). The 53 μm-CHF particles may constitute filler obstacles for water vapor diffusion across the composite matrices, and also probably decreased the swelling capacity of the LMP matrix. Also, CHF concentrations above 1% can decrease the water vapor solubility in the composites. According to Spence, Venditti, Rojas, Pawlak and Hubbe (2011), increasing sample crystallinity, as occurred in the CHF-composites (Fig. 5C), should reduce the WVP.

Abdollahi, Alboofetileh, Rezaei, & Behrooz (2013) developed by casting alginate films (25% glycerol, polymer basis) reinforced by cellulose nanowhiskers. The tensile strength at failure increased from 18 MPa for 0%-alginate films to 22 MPa for 5%-nanowhisker film, but decreased again to 18 MPa for 10%-nanowhisker film. A maximal Young's modulus of 300 MPa was observed for the 5%-nanowhisker film. This behavior was similar to that obtained for CHF-LMP films, but notably higher strength was observed in 5%-CHF-LMP films (Fig. 6A). Simultaneously, Abdollahi et al. (2013) determined that the elongation decreased from 12% to 8% with the rise from 0% to 5% in the cellulose nanowhisker concentration, while increased to 10% for a higher nanowhisker level (10% w/w). The WVP of films, measured against the 1.5%–100% RH gradient at 20 °C, decreased from 2.0×10^{-10} to 1.68×10^{-10} g m^{-1} s^{-1} Pa^{-1} for nanoparticle concentrations increasing from 0% to 3%, whereas the WVP (1.65×10^{-10} g m^{-1} s^{-1} Pa^{-1}) did not change for concentrations between 3% and 10%. This WVP results were not corrected by the Gennadios et al. (1994) method, which leads to increased final values of WVP.

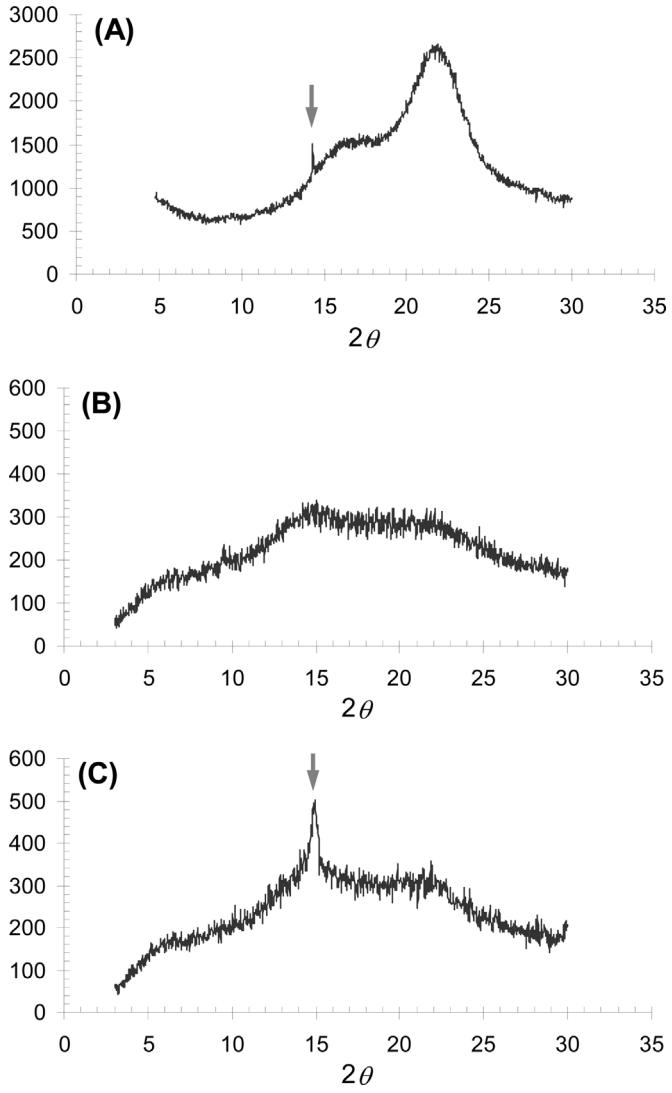

Fig. 5. X-ray diffraction patterns obtained from CHF powder (A) as well as from 0%- (B) and 5%- (C) CHF-LMP composites.

3.4.4. Contact angle

The contact angle was determined at the film surface through a sessile water drop deposited on the film. All values obtained were below 90° (Table 3) and, hence, the liquid is said to wet the film. The only contact angle that was significantly ($p < 0.05$) higher than the rest was that corresponding to the 5%-CHF film. Hence, the critical particle volume fraction at which the particles could form an interconnected network seemed also to diminish the hydrophilicity of the film surface. The difference between values was also maintained at 60 s of water drop permanence (Table 3). A surface tension of 0.061 J/m^2 can only be calculated from the contact angle recorded at 5 s for the 5%-CHF film, according to the TAPPI 565 pm-96 standard (1996), and hence can be equivalent to a surface treatment for films used in packaging.

3.4.5. Antioxidant capacity of films

The antioxidant capacity of films was evaluated as the radical scavenging (DPPH assay) and reducing (FRAP technique) activities. Some significant scavenging capacity was only detected for the 8% fiber loaded film, which coincided with the highest total phenolic content determined in films. On the other hand, the reducing activity increased significantly ($p < 0.05$) when the fiber content of films rose from 1% to 5% or to 8%, which in general paralleled the

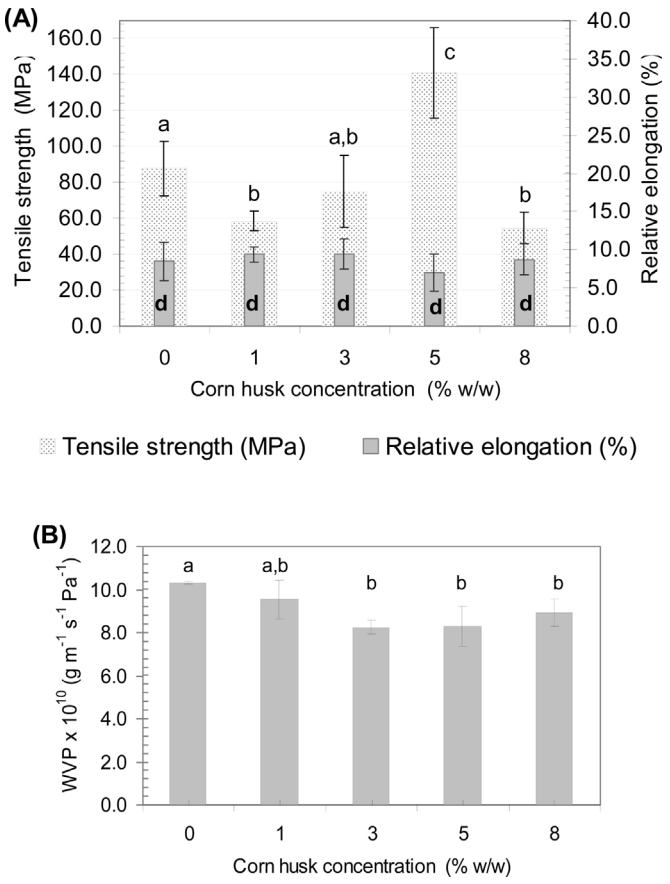

Fig. 6. Tensile strength and relative elongation (A) at film failure, as well as WVP of films (B) plotted against CHF concentration. Error bars indicate the standard deviation ($n = 14$ for tensile assays; $n = 3$ for WVP). The same letters for a given parameter mean non significant differences ($p < 0.05$).

total phenolic contents in films (Table 4). Phenolics increased significantly ($p < 0.05$) with the CHF level in films (Table 4). CHF was constituted by the cell wall polysaccharides, as above described, which also showed a 2.64% w/w of phenolics (Bernhardt et al., 2015). CHF herein used for the composite films also contained carotenes (5.74 mg/100 g of dried fiber) (Bernhardt et al., 2015), which can also contribute to the antioxidant activity of composites.

4. Conclusions

Chemical composition of the water insoluble fiber (CHF) extracted from the corn husk residue (69% w/w yield), characterized by an important content of arabinoxylans and a low content of pectins, together with a 32% of crystallinity, justified a less hydrophilic behavior of CHF. Hence, the 53 μm-CHF was then evaluated at 0, 1, 3, 5, 8% w/w concentrations for decreasing WVP and improving mechanical strength and surface properties.

Homogeneous films were obtained, with a continuous, smooth and compact LMP matrix filled by CHF (tubes and irregular shaped fibers), which produced a continuous but waved surfaces. FTIR analysis of composite films showed essentially the LMP spectrum. Glass transition temperatures indicated that amorphous rubber composite films were obtained due to the LMP matrix, though amorphous glassy regions were also found, associated to the CHF filler. The fiber presence also increased in ≈10 °C the onset of thermal decomposition of films.

The 5% w/w was found to be the critical concentration of CHF that constituted a biopolymeric composite film where fiber microparticles (53 μm mean size) can probably form an inter-

connected network that strengthened, without significant loss of deformability, the calcium-crosslinked LMP matrix of film, while constituted a better barrier to water vapor than 0%-CHF LMP film. An important loss of hydrophilicity was also produced at the film surface, as demonstrated by the significant contact angle increase to 44°, from low values obtained (25°) from the 0%-CHF LMP film. At the same time, 5% w/w CHF film showed a significant antioxidant (reducing) capacity (25 mg ascorbic acid/100 g film) associated to the co-extracted phenolics and carotenes of the CHF loaded.

Corn husk residue with co-extracted natural antioxidants can be utilized as a source of fibers for material development such as composite films with enhanced performance, which can constitute an antioxidant barrier at food interfaces.

Acknowledgements

This work was supported by the University of Buenos Aires [grant number 2014-2017 20020130100553BA], National Research Council of Argentina (CONICET) [grant number 2012-2014 PIP 112-201101-00349] and ANPCyT [grant number 2014-2017 PICT 2013-2088]. We thank Carlos Rozas (INTI-Celulosa y Papel, Buenos Aires, Argentina).

References

Abdollahi, M., Alboofetileh, M., Rezaei, M., & Behrooz, R. (2013). Comparing physico-mechanical and thermal properties of alginate nanocomposite films reinforced with organic and/or inorganic nanofillers. *Food Hydrocolloids*, *32*, 416–424.

Andrade, R. M. S., Ferreira, M. S. L., & Gonçalves, E. C. B. A. (2016). Development and characterization of edible films based on fruit and vegetable residues. *Journal of Food Science*, *81*(2), E412–E418.

Assifaoui, A., Loupiac, C., Chambin, O., & Cayot, P. (2010). Structure of calcium and zinc pectinate films investigated by FTIR spectroscopy. *Carbohydrate Research*, *345*(7), 929–933.

Basanta, M. F., Marin, A., De Leo, S. A., Gerschenson, L. N., Erlejman, A. G., Tomas-Barberan, F. A., et al. (2016). Antioxidant Japanese plum (*Prunus salicina*) microparticles with potential for food preservation. *Journal of Functional Foods*, *24*, 287–296.

Bernhardt, D. C., Ponce, N. M. A., Stortz, C. A., & Rojas, A. M. (2015). Análisis químicos y fisicoquímicos de brácteas de Zea mays L. y de sus polisacáridos de pared celular. In *XX simposio nacional de química orgánica, soc. Argentina de investigación en química orgánica*.

Braccini, I., & Pérez, S. (2001). Molecular basis of Ca^{2+}-induced gelation in alginates and pectins: The egg box model revisited. *Biomacromolecules*, *2*, 1089–1096.

Brand-Williams, W., Cuvelier, M. E., & Berset, C. (1995). Use of free radical method to evaluate antioxidant activity. *LWT—Food Science and Technology*, *28*, 25–30.

Coimbra, M. A., Barros, A., Barros, M., Rutledge, D. N., & Delgadillo, I. (1999). FTIR spectroscopy as a tool for the analysis of olive pulp cell-wall polysaccharide extracts. *Carbohydrate Research*, *317*, 145–154.

De'Nobili, M. D., Pérez, C. D., Navarro, D. A., Stortz, C. A., & Rojas, A. M. (2013). Hydrolytic stability of L-(+)-ascorbic acid in low methoxyl pectin films with potential antioxidant activity at food interfaces. *Food and Bioprocess Technology*, *6*, 186–197.

Dhugga, K. S. (2007). Maize biomass yield and composition for biofuels. *Crop Science*, *47*, 2211–2227.

Fang, J. M., Sun, R. C., & Tomkinson, J. (2000). Isolation and characterization of hemicelluloses and cellulose from rye straw by alkaline peroxide extraction. *Cellulose*, *7*, 87–107.

Fissore, E. N., Santo Domingo, C., Pujol, C., Damonte, E., Rojas, A. M., & Gerschenson, L. N. (2014). Upgrading of residues of bracts, stems and hearts of *Cynara cardunculus* L. var. scolymus to functional fractions enriched in soluble fiber. *Food & Function*, *5*, 463–470.

Galanakis, C. M. (2013). Emerging technologies for the production of nutraceuticals from agricultural by-products: A viewpoint of opportunities and challenges. *Food and Bioproducts Processing*, *91*, 575–579.

Gennadios, A., Weller, C. L., & Gooding, C. H. (1994). Measurement errors in water vapor permeability of highly permeable, hydrophilic edible films. *Journal of Food Engineering*, *21*, 395–409.

Greenspan, L. (1977). Humidity fixed points of binary saturated aqueous solutions. *Journal of Research of the National Bureau of Standards–A. Physics and Chemistry*, *81A*(1), 89–96.

Hatakeyama, H., & Hatakeyama, T. (1998). Interaction between water and hydrophilic polymers. *Thermochimica Acta*, *308*, 3–22.

Huang, F. Y. (2012). Thermal properties and thermal degradation of cellulose tri-stearate (CTs). *Polymers*, *4*, 1012–1024.

Huq, T., Salmieri, S., Khan, A., Khan, R. A., Le Tien, C., Riedl, et al. (2012). Nanocrystalline cellulose (NCC) reinforced alginate based biodegradable nanocomposite film. *Carbohydrate Polymers*, *90*, 1757–1763.

Idrovo Encalada, A. M., Basanta, M. F., Fissore, E. N., De'Nobili, M. D., & Rojas, A. M. (2016). Carrot fiber (CF) composite films for antioxidant preservation: Particle size effect. *Carbohydrate Polymers*, *136*, 1041–1051.

Larrauri, J., Rupérez, P., & Saura-Calixto, F. (1997). Mango peel fibres with antioxidant activity. *European Food Research and Technology*, *205*, 39–42.

Lavelli, V., & Kerr, W. (2012). Apple pomace is a good matrix for phytochemical retention. *Journal of Agriculture and Food Chemistry*, *60*, 5660–5666.

Liu, Y., Bandhari, B., & Zhou, W. (2006). Glass transition and enthalpy relaxation of amorphous food saccharides: a Review. *Journal of Agriculture and Food Chemistry*, *54*, 5701–5717.

Olagunju, A., Onyike, E., Muhammad, A., Aliyu, S., & Abdullahi, A. S. (2013). Effects of fungal (*Lachnocladium spp.*) pretreatment on nutrient and antinutrient composition of corn cobs. *African Journal of Biochemistry Research*, *7*(11), 210–214.

Pérez, C. D., De'Nobili, M. D., Rizzo, S. A., Gerschenson, L. N., Descalzo, A. M., & Rojas, A. M. (2013). High methoxyl pectin-methyl cellulose films with antioxidant activity at a functional food interface. *Journal of Food Engineering*, *116*, 162–169.

Ping, Z. H., Nguyen, Q. T., Chen, S. M., Zhou, J. Q., & Ding, Y. D. (2001). States of water in different hydrophilic polymers-DSC and FTIR studies. *Polymer*, *42*(20), 8461–8467.

Pulido, R., Pulido Bravo, L., & Saura-Calixto, F. (2000). Antioxidant activity of dietary polyphenols as determined by a modified ferric reducing/antioxidant power assay. *Journal of Agricultural and Food Chemistry*, *48*, 3396–3402.

Ramos, O. L., Reinas, I., Silva, S. I., Fernandes, J. C., Cerqueira, M. A., Pereira, R. N., et al. (2013). Effect of whey protein purity and glycerol content upon physical properties of edible films manufactured therefrom. *Food Hydrocolloids*, *30*, 110–122.

Shekarabi, A. S., Oromiehie, A. R., Vaziri, V., Ardjmand, M., & Safekordi, A. A. (2014). Investigation of the effect of nanoclay on the properties of quince seed mucilage edible films. *Food Science & Nutrition*, *2*(6), 821–827.

Shi, H. (2001). Introducing natural antioxidants. In J. Pokorny, N. Yanishlieva, & M. Gordon (Eds.), *Antioxidants in foods*. Cambridge: CRC Press, Woodhead Publishing Limited. Practical applications (pp.149).

Shui, G., & Leong, L. P. (2006). Residue from star fruit as valuable source for functional food ingredients and antioxidant nutraceuticals. *Food Chemistry*, *97*, 277–284.

Singh, T. P., Chatli, M. K., & Sahoo, J. (2015). Development of chitosan based edible films: Process optimization using response surface methodology. *Journal of Food Science and Technology*, *52*(5), 2530–2543.

Spence, K. L., Venditti, R. A., Rojas, O. J., Pawlak, J. J., & Hubbe, M. A. (2011). Water vapor barrier properties of coated and filled microfibrillated cellulose composite films. *BioResources*, *6*(4), 4370–4388.

TAPPI 565 pm-96 standard. (1996). *Contact angle of water droplets on corona-treated polymer film surfaces*.

Träubel, H. (1999). Hydrophilic polymers. In H. Träubel (Ed.), *New materials permeable to water* (pp. 134–135). Berlin: Springer-Verlag.

Uhlin, K. I., Atalla, R. H., & Thompson, R. S. (1995). Influence of hemicelluloses on the aggregation patterns of bacterial cellulose. *Cellulose*, *2*, 129–144.

Wessling, B. (1991). Electrical conductivity in heterogeneous polymer systems. V (1): Further experimental evidence for a phase transition at the volume concentration. *Polymer Engineering & Science*, *31*(16), 1200–1206.

Wilson, R. H., Smith, A. C., Kačuráková, M., Saunders, P. K., Wellner, N., & Waldron, K. W. (2000). The mechanical properties and molecular dynamics of plant cell wall polysaccharides studied by Fourier-transform infrared spectroscopy. *Plant Physiology*, *124*, 397–405.

Xiao, L. P., Sun, Z. J., Shi, Z. J., Xu, F., & Sun, R. C. (2011). Impact of hot compressed water pretreatment on the structural changes of woody biomass for bioethanol production. *BioResources*, *6*(2), 1576–1598.

Yang, J., Yu, J., & Ma, X. (2006). Study on the properties of ethylenebisformamide and sorbitol plasticized corn starch (ESPTPS). *Carbohydrate Polymers*, *66*, 110–116.